Applied Nanoscience
https://doi.org/10.1007/s13204-023-02988-y

ORIGINAL ARTICLE

2D material graphene as a potential antidiabetic and nontoxic compound in *Drosophila melanogaster*

Kalpanarani Dash[1] · Deepak kumar Panda[1] · Kushal Yadav[1] · Sonali Meher[1] · Monalisa Mishra[1]

Received: 15 September 2023 / Accepted: 23 November 2023

Abstract

This study explains the potential role of non-functionalized graphene produced using flash joule heating technology on *Drosophila melanogaster*. Several characterizations of the produced graphene were conducted via field emission-scanning electron microscopy, high-resolution transmission electron microscopy, Raman spectroscopy, and X-ray diffraction studies. After being characterized, the graphene powder was orally administered to flies at doses ranging from 0.02 to 0.5%, establishing its non-toxic properties as a prerequisite for potential therapeutic applications. Experiments such as Trypan blue and 4',6-diamidino-2-phenylindole (DAPI) revealed that graphene causes no harm to the larval gut's plasma membrane and nucleus. Behavioral assays such as crawling and climbing assays on larvae and adults demonstrated the non-neurotoxic nature of graphene. The high sucrose diet-induced diabetic *Drosophila melanogaster* model was used to study antidiabetic properties. In contrast, Gram + ve bacteria *B. subtilis* and Gram − ve *P. aeruginosa* were used to study the antibacterial properties of graphene. A better metabolic profile was evidenced after graphene treatment, including a 36% decrease in hemolymph-free glucose levels and significantly reduced lipid droplets at the highest concentration. In addition, the highest concentration of graphene treatment resulted in a 57% reduced fluorescent intensity of reactive oxygen species (ROS) produced by diabetic flies. Considering all these evidence, this study concludes that graphene's non-toxic and antidiabetic properties can be used to mitigate the symptoms associated with Type II diabetes and obesity.

Keywords 2D materials · Antidiabetic properties · *Drosophila* · Graphene · Neurotoxicity · Obesity

Introduction

Two-dimensional (2D) materials are known for their extremely thin nature, typically measuring only a few nanometers or less. A better surface area and exceptional electrical conductivity are two of the key characteristics of these materials, which make them effective for generating analytical sensors. Because of their fast reaction times and cost-effectiveness, electrochemical sensor-based 2D materials have recently been propounded for monitoring several biological compounds, food additives, pharmaceuticals, and environmental contaminants (Karimi-Maleh et al. 2022; Tabrizi et al. 2022; Vatandost et al. 2021; Zabihpour et al. 2020). Electrons within two-dimensional (2D) materials can freely navigate within a two-dimensional plane, unlike three-dimensional (3D) materials. Currently, the category of 2D materials encompasses numerous crystals. In addition to the well-known graphene, graphene oxide (Salimbahrami et al. 2023; Seyedi et al. 2023; Sharif Nasirian et al. 2021; Vatandost et al. 2021), and reduced graphene oxide (GO/rGO)(Yan et al. 2010), they also include hexagonal boron nitrite (h-BN)(Cartamil-Bueno et al. 2017), graphene (Elias et al. 2009), fluorographene (Nair et al. 2010), transition-metal dichalcogenides (TMDCs) (X. Li and Zhu 2015), and 2D metal oxides such as $Bi_2Sr_2CaCu_2Ox$ (Novoselov et al. 2005), graphitic carbon nitrite (g-C_3N_4) (Dong et al. 2014), black phosphorus (BP) (Jiang and Park 2014), and germanene (Ni et al. 2012). The hexagonal configuration of a graphene monolayer has captured researchers' interest across various fields, spanning biosensors, microelectronics, composite materials, supercapacitors, and medicinal applications (Tiwari et al. 2016; Tiwari et al. 2018; Y. Yang et al. 2015). In graphene, every carbon atom is sp^2 hybridized, with a characteristic C–C bond distance of 0.142 nm. Graphene

✉ Monalisa Mishra
mishramo@nitrkl.ac.in

[1] Neural Developmental Biology Lab, Department of Life Sciences, National Institute of Technology, Sundergarh, Rourkela,, Odisha 769008, India

Published online: 23 January 2024

exhibits a unique electronic cloud that tightly binds each carbon atom to its neighboring atoms by covalent bonding (Hughes and Walsh 2015; Liao et al. 2014; Tiwari et al. 2018). Apart from this, graphene also has excellent thermal and electrical conductivity.

A burdensome task in modern chemistry is a large-scale, low-cost, and environmentally friendly synthesis of graphene as a monolayer sheet of carbon. Graphene is commonly synthesized via (1) chemical reduction, (2) mechanical cleavage from natural graphite, (3) electrochemical exfoliation, (4) liquid phase exfoliation, (5) chemical vapor deposition, and (6) epitaxial growth (Abbas et al. 2022; Peng et al. 2015; Zhang et al. 2017). rGO is synthesized chemically from graphite by oxidizing, reducing, and centrifuging. The toxicity of the reducing agents used here, such as hydrazine, is a serious problem for large-scale manufacturing (Chandu et al. 2017; Chekin et al. 2016; Vatandost et al. 2020a, b). However, it was recently synthesized via flash joule heating (FJH) using coal, discarded food, rubber tires, plastic wastes, carbon black, etc. The graphene synthesized by this method is known as flash graphene (FG). The FG synthesis procedure precludes using a furnace, solvents, reactive gases, or any hazardous reducing agents. The purity of the product depends on the source material's carbon content. A high-voltage electric discharge generated from a capacitor bank that produces temperatures surpassing 3,000 K in less than 100 ms is used in this procedure. After such rapid heating, amorphous carbon is transformed into a turbostratic arrangement, forming the layers of flash graphene (FG) (Luong et al. 2020). As a result, the likelihood of contaminants is minimized, ensuring the purity of the final product.

Graphene nanoplates (GNPs) are used in carbon nanofillers, which are now being implemented to enhance the mechanical performance of different thermoplastic polymer-based biocomposites. Thermal-modified 3D graphene prepared by wet chemical exfoliation shows increased antioxidant and hemolysis rates when comes in contact with blood (Kaczmarek-Szczepańska et al. 2023; Kamedulski et al. 2021; Rouway et al. 2021). In this way, graphene and its derivatives offer distinct and innovative prospects for the advancement of novel biosensors. The successful detection of crucial biomolecules within a cellular environment, including nucleic acids (Mohanty and Berry 2008), proteins (Ohno et al. 2010), growth factors (Chen et al. 2012), hormones (Pu et al. 2011), adenosine triphosphate (ATP) (He et al. 2011), fungal toxins (Sheng, Ren, Miao, Wang, and Wang, 2011), as well as various harmful metals such as mercury (Hg) (Huang et al. 2011), silver (Ag) (Wen et al. 2010), and copper (Cu) (Liu et al. 2011), has been effectively showcased through the utilization of biosensor made using graphene and its derivatives that have been suitably functionalized. The detection of live cell caspase-3 activity can also be achieved through the utilization of GO (H. Wang et al. 2011). Graphene exhibits biocompatibility and favorable electrical conductivity, making it suitable for various applications such as siRNA delivery (De Lázaro et al. 2019), pH-responsive small-molecule drug delivery (Yang et al. 2008), and stem cell culture (Park et al. 2011).

Graphene oxide is another functionalized graphene that may also be used as an adsorbent in the heavy metal and organic compound adsorption processes. It is an excellent adsorbent overall because of its several functional groups, which include hydroxyl (OH), alkoxy (C–O–C), carbonyl (C=O), and carboxyl (COOH). Due to its high conductivity, graphene oxide finds extensive use in biomedicine, electronics, solar desalination, antibacterial coating, anticancer agents, sensors, and photocatalysis. Drug loading matrices employ graphene's porous carbon structure, which provides a large surface area and variable pore size for drug delivery (Salimbahrami et al. 2023; Seyedi et al. 2023; Sharif Nasirian et al. 2021; Vatandost et al. 2021).

Another kind of graphene that has various benefits is reduced graphene oxide (rGO), which makes it a better candidate for use as a drug delivery vehicle. In electrochemical sensing, GO-based nanocomposite serves as a magnetically controlled material. Electrochemical sensors based on magnetic graphene nanocomposite have demonstrated high sensitivity and a linear range spanning many orders of magnitude. Previous research indicates that Fe_3O_4–rGO exhibits potent antibacterial, antioxidant, and anticancer properties. When used in practical sample analysis, graphene/magnetic graphene nanocomposite has considerable promise for developing high-performance electrochemical sensors. A susceptible electrochemical sensor called rGO-modified carbon paste electrode (rGO/CPE) was employed to detect the food additive known as sunset yellow in food. Potential antioxidant, antibacterial, and anticancer effects are present in green-synthesized graphene such as green tea extract-reduced graphene oxide (Abdi et al. 2020; Behrouzifar et al. 2021; Tabrizi et al. 2022; Vatandost et al. 2020a, b; Vatandost et al. 2020a, b). Graphene nanosheets, modified with various surface modifiers such as polyethylene glycol (PEG), are widely employed in cellular gene delivery applications.

Every health care-related research mentioned above that has used graphene necessitates either some hybridization or the production of nanocomposites. The chemical synthesis procedures often include multiple steps and are costly enough. Moreover, the compound's durability and suitability raise a major concern before being used in living cells. As a groundbreaking approach, our study introduces flash joule-heated pure graphene as a therapeutic compound for the model organism *Drosophila melanogaster*. In particular, this approach eliminates the need for additional functionalization or hybridization. While being administered orally, this graphene exhibits significant hypoglycemic, antiobesity,

antioxidant, and antibacterial properties. This underscores the novelty and significance of our work.

Drosophila melanogaster, an invertebrate model, is easily raised and cultured in laboratories with limited space. Their low maintenance cost makes them even more ideal for scientific studies. The whole-sequenced genome, transcriptomes, proteome, 60% of genome homology, presence of less duplicated genes, and 75% of disease gene homology with humans add more advantages. It is now possible to mutate the fly genome to produce transgenic animals for studying the pathophysiology of several human diseases, such as Parkinson's disease, Alzheimer's disease, heart disease, Friedrich's ataxia, aging, cancer, and metabolic disorders such as diabetes. Furthermore, substances consumed by humans, including cocaine, methamphetamine, caffeine, alcohol, nicotine, and cannabis, have all been studied using *Drosophila*. The current study aims to decipher graphene's nontoxic properties and biological application using *Drosophila melanogaster.*

Materials and methods

The purest forms of flash graphene nanosheet (1–3) layers were obtained from Graphenera. Carbon Pvt. Ltd. It resembles the structure of pristine graphene. This is basically a hexagonal carbon plane sheet synthesized by the flash joule heating method. The compound has a particle size of 20–200 nm; the surface area is > 400 m^2g obtained from BET analysis. There is also an electrical conductivity of > 105 Sm^{-1}, a thermal conductivity of > 3000 Wm^{-1} k^{-1}, and a bulk resistivity of < 0.1 Ω^{-cm}.

Characterization of graphene

The working principle of FE-SEM relies on the liberation of primary electrons from a source of field emission and accelerated in a high electric field. Electronic lenses further deflect these primary electrons, producing a narrow scan beam of that object. As a result, secondary electrons are emitted from every spot on the surface of the object. These electrons are trapped by a detector, and an electronic signal is produced. The surface morphology of the graphene was analyzed using a Supra 55 (Carl Zeiss, Germany) field emission-scanning electron microscope (FE-SEM) at 5–10 kV and a Thermo Scientific high-resolution transmission electron microscope (HR-TEM) (Talos F200X G2). The UV–vis spectra of the graphene powder were recorded on a JASCO V-650 spectrophotometer attached to a $BaSO^4-$ coated integration sphere. The crystallographic structure of graphene was analyzed using a X-ray diffractometer-Texture (Bruker, Cobalt-k-α) at a scanning rate of 5°/min, 2θ range (5–100)°, and a step size of 0.02.

An energy dispersive X-ray spectroscopy (EDS)-based scanning electron microscope (SEM) is used to analyze a compound's chemical features. The primary operating principle that enables SEM-EDS to function is the capacity of high-energy electromagnetic radiation (X-rays) to eject "core" electrons (electrons that are not in the outermost shell) from an atom. After removing primary electrons, the system will be left with a hole that a higher-energy electron can fill, and while doing this, the high-energy electrons release some energy. The energy released by this process is specific for every element on the periodic table. In this way, we can predict what elements are present and in what proportion they are present. Signals produced in an SEM-EDS system include secondary and backscattered electrons used in image forming for morphological analysis and X-rays used for identifying and quantifying chemicals present at detectable concentrations. To study the structural constituents of the graphene used in our study, we have used SEM-EDS (JEOL-JSM-6480-LV).

Fly maintenance and generation of diabetic fly

Out of several species of *Drosophila*, *D. melanogaster, Oregon. R* strains were selected for all the experiments. To induce Type II diabetes, flies were grown under a high-sugar diet containing 35% sucrose (HiMedia GRM601), 5% corn meal, 2.5% yeast (fermenting agent), and 1% Type-1 Agar (HiMedia GRM666). Further addition of methylparaben and propionic acid makes it free from fungal and bacterial contamination. Flies were kept in standard laboratory conditions at 22°C, 12 h of alternative light–dark conditions, and 60–70% humidity.

Preparation of graphene stock solution

To prepare a stable graphene solution without dispersants or surfactants is quite challenging due to the hydrophobic characteristics of graphene. Graphene was dispersed in a mixed solution of DMSO. Graphene powder was mixed with distilled water containing 0.8% DMSO (as it has been reported earlier that DMSO at a concentration of 0.8% is nontoxic to *Drosophila*), followed by 30 min of bath sonication to prepare a 1% stock solution (10 mg/ml).

Presence of graphene within the gut

Six adult *Drosophila melanogaster* were fed with 150 µl (0.02%), 250 µl (0.05%), and 500 µl (0.5%) of graphene for 7 days, followed by gut dissected under a stereomicroscope (Motic—SMZ 171) with the help of a sharp-end forceps and a needle. Then, they were placed over a clean glass slide and mounted using 20% glycerol. Finally, structural characterization was done. Raman spectroscopic analysis was done

using a PL Micro Raman Spectrometer (alpha 300R, WITec) at a wavelength of 500–4000 nm to detect the presence of graphene in the foregut and midgut.

Toxicity assessment

To check the toxic effect of graphene in flies, we performed several experiments in both larvae and adults. We checked the toxicity of graphene by feeding it to *Drosophila* through diet. We had four different types of food medium: one standard food medium and the other three food mediums contained three different graphene concentrations: 0.5%, 0.05%, and 0.02%. Flies were grown under these mediums from the egg to the adult stage, and the toxicity of graphene was checked in both larvae and adults.

Toxicity of graphene to the larval gut

DAPI staining Ten larval guts from each experimental setup were isolated and fixed with PFA overnight. To discard the fixative, washing the sample with 1X PBS multiple times was considered, and for better dye penetration, the samples were further incubated with 1% PBST for 20 min in two series. Five microliters of DAPI (D9542, Sigma-Aldrich, Merck, Germany) at a working solution of 1 µg/ml was added to stain the sample for 5 min in the dark. The mounting procedure was done using 20% glycerol on a clean slide (Kumar et al. 2023), and the final images were taken under the same confocal microscope (Leica DMI8).

Trypan blue dye exclusion assay Briefly, 5–6 larvae at their 3rd instar stage from the control and each graphene-treated vial were taken and washed correctly with phosphate-buffered saline to remove all the food residues. Then, the larvae were submerged in 0.2% trypan blue solution (93,595, Sigma-Aldrich, Merck, Germany) in a 1.5-ml Eppendorf tube and kept in the dark in shaking condition for 30 min. After incubation, the dye was discarded, and the larvae were properly washed 3–4 times in 1 × PBS to clean all the background stains to see the gut inside the transparent larvae. Images of the larvae were taken under a stereo microscope (Murmu et al. 2023) (MOTIC SMZ171).

The neurotoxicity of graphene nanoparticles was tested via two different experiments.

Crawling assay of 3rd instar larvae For the crawling assay, 6–7 third instar larvae were extracted from the control and all the graphene-treated food vials. All the larvae were properly rinsed using PBS. Subsequently, the larvae were permitted to move sequentially, positioned at the central region of an agar plate with a concentration of 2%. The duration of each larva's journey from the center to the periphery was documented using a camera (Canon EOS 3000D, Japan), and the crawling path of each larva was drawn on the back side of the agar plate with the help of a marker (P. Nayak et al. 2023).

Climbing assay of adult flies Adult flies have an inherent ability to climb against gravity. Twenty-five adult flies from both the control and experimental setup were taken. The adult flies were placed inside a transparent plastic cylinder without anesthetizing them. The plastic cylinder's open end was closed with a cotton plug. The cylinder containing flies was tapped 3–5 times against a spongy surface to bring all the flies toward the bottom, and then in an interval of 10 s, the number of flies able to climb 50% length of the cylinder and 80% length of the cylinder was noted. The percentage of climbers and non-climbers was calculated. The process was repeated three times with a break of 30 s after every climb to obtain the mean rate, and each experiment was done in triplicate (Mishra 2020).

Phenotype check

Eye, wings, thorax, abdomen, and adult body phenotypes of flies after being reared in graphene-treated food medium at different concentrations were checked and compared with the phenotype of the control flies. All the images were taken under a stereo microscope (Motic SMZ171).

Experiments to elucidate the antidiabetic properties of graphene

We selected diabetic flies as our experimental model and administered graphene at a non-toxic concentration to investigate its antidiabetic potential in these flies. 0.5%, 0.05%, and 0.02% graphene working solutions were added to the traditional food (5% sucrose, 5% cornmeal, 2.5% yeast, and 1% agar) to study its antiobesity and antidiabetic properties. In the case of *Drosophila*, flies grown and hatched in a high-sugar diet medium were obese and had high circulating sugar in their hemolymph. After 10–12 days, adult diabetic flies and control flies were transferred to the respective graphene-containing food and standard food media after the food was solidified, with a male–female ratio of 3:5. After 7 days of graphene feeding, the same adult flies were taken for several experiments. We have also transferred some diabetic flies to the traditional food medium without graphene to confirm that the antiobesity and antidiabetic effects were only because of graphene and not due to the change of food from a high-sugar diet to a regular diet.

Several experiments were performed to prove the antidiabetic properties of graphene. All these experiments had four setups (the first one contained 10–12-day-adult diabetic flies, the second one had 10–12-day-old adult control flies,

the third one had adult diabetic flies treated under three different concentrations of graphene in a control medium for 7 days, and the fourth setup contained diabetic flies transferred to control food medium for 7 days).

Developmental cycle study

The development of *Drosophila* in five different diet media was studied, such as in standard food medium, high-sugar medium, and three different concentrations of graphene-treated food medium (0.5%, 0.05%, and 0.02%). Virgin male and female diabetic flies were transferred to three other graphene food mediums and the HSD medium adults at a male–female ratio of 5:7. On the one side, the same adult nondiabetic flies in a percentage of 5:7 were transferred to the standard medium and taken as a reference. The vials were observed every 6 h to detect developmental changes from the day of parental transfer to the day of emergence of 1st adult fly (Mishra 2020). The graph was plotted based on the time taken in hours to convert from one developmental stage to another.

Pupal count

At a time duration of every 6 h, the number of 3rd instar larvae converted into pupa was also calculated. The experiment was continued for 3 days, and the number of pupae formed in the 1st, 2nd, and 3rd days was also compared in different food mediums (Mishra 2020).

Free glucose estimation

Ten adult flies (five males and five females) were taken from each experimental setup. The flies were homogenized by adding 100 µl of ice-cold PBS using a micro pestle inside a 1.5-ml Eppendorf tube in a mini cooler at a temperature of − 20 ℃. The homogenates were 1st centrifuged at 4 ℃ at 5000 rpm for 5 min. Clear supernatants were collected and heat-inactivated for 10 min at 70 ℃ and finally, centrifugation was done at 12,000 rpm for 3 more minutes. Twenty microliters of hemolymph was collected from the final supernatant diluted with 1X PBS at a 1:4 ratio to obtain the final volume of 100 µl. Glucose standards were previously prepared from 1 mg/ml stock as 0.16 mg/ml, 0.8 mg/ml, 0.4 mg/ml, 0.2 mg/ml, and 0.1 mg/ml. Thirty microliters of all the standard solutions and the samples was added to a 96-well plate in triplicate, and 100 µl of glucose oxidase/peroxidase reagent was added to each well for the enzymatic reaction and incubated at 37 ℃ for 1 h. After 1 h, 12N H_2SO_4 was poured into each well to terminate the reaction, and absorbance was reported at 540 nm. Glucose oxidase reacts with D-glucose and converts it into d-gluconic acid. Peroxidase converts oxidized o-dianisidine to reduced o-dianisidine, which gives a brown color, after adding H_2SO_4, which converts it to a pink color, indicating termination of the enzymatic reaction (Mukherjee et al. 2022).

Nile red staining

Ten adult flies from the control and each experimental vial were taken to detect the phospholipid amount in the gut, and the guts were dissected. Unfixed gut samples were incubated in 20–30 µl of Nile red working solution (1 µg/ml) and 10 µl of 20% glycerol in the dark for 1 h. After incubation, the gut samples were properly rinsed 2–3 times using 1X PBS and mounted using 20% glycerol and putting a coverslip. Bright red lipid droplets were seen all over the gut under the confocal microscope (Leica DMI8) (N. Nayak and Mishra 2021).

ROS detection

DCFH-DA assay In the DCFH-DA assay, we took five adult flies, including control, graphene treated, and diabetic flies. We took ten adult flies from each setup, dissected their gut, and fixed them in 4% PFA overnight. The next morning, we carried forward the staining of the gut sample after discarding the PFA, followed by several washing steps using 1X PBS (3 times) and 1% PBST (2 times) for better dye penetration. We incubated the gut sample with 20 µl of DCFH-DA dye (D6883, Sigma-Aldrich, Merck, Germany) at 1 µg/ml working concentration for 30 min, covering with an aluminum foil and avoiding light. Subsequently, the dye was disposed of, and the samples underwent three washes using 1 × phosphate-buffered saline (PBS). We mounted them separately for imaging the gut sample following the mounting procedure of the DAPI staining explained above (Kumar et al. 2023). Images were taken via a confocal microscope (Leica DMI8).

Antibacterial activity of graphene

One hundred and forty microliters of LB broth (HiMedia-M1245) and 10 µl of inoculum of *Pseudomonas aeruginosa* (10^5 cfu/ml) were taken in one well of a sterile 96-well plate and taken as control. Similarly, another well was poured with 140 µl of LB broth and 10 µl of *Bacillus subtilis* (10^5 cfu/ml) as control. Two milliliter solutions of each of 1%, 10%, and 100% of graphene were prepared by dissolving them in PBS and 0.8% DMSO. Then, 50 µl of each graphene solution was taken in three different wells containing 140 µl of LB broth and 10 µl of inoculum of *P. aeruginosa*. The same steps were followed for *B. subtilis*. The 96-well plate was then incubated inside a BOD incubator, and then reading was taken with the help of a microplate reader (Genetix, Biotech Asia Pvt. Ltd.) at 0 h, 6 h, 12 h, 18 h, and 24 h. The graph was plotted with the help of GraphPad Prism 5.

Statistical analysis

We analyzed all experimental data using the software GraphPad Prism 5.0. Using the significance $*P<0.05$, $**P<0.01$, and $***P<0.001$ from paired two-tailed Student's *t*-test, and for grouped data, we used a two-way ANOVA test. The data were interpreted with the mean ± SEM values.

Results and discussion

Because of their fascinating physiochemical features, graphene and its derivatives have long been used as a substance of considerable interest. It is emerging as a key component in the field of biomedical applications as a biosensor, a drug, a gene delivery agent, and a tool for tumor cell imaging, cancer, and photothermic applications. After finding a place in industries as a potential candidate for various applications in nanoelectronics, energy technologies, and fuel cells, recent research has begun to concentrate on graphene's involvement in living systems, following the oral delivery of graphene oxide to living organisms and subsequent studies of its effects. According to previous research, significant behavioral and developmental abnormalities were observed in *Oregon-R* flies when fed with graphene oxide (GO) at higher concentrations of 50–300 µg/ml (Priyadarsini et al. 2019). According to a different investigation, the W^{1118} strain exhibited notable toxicity upon exposure to GO (Guo et al. 2022). GO at a concentration of 0.02–1%, when fed to *Drosophila*, improves their metabolic profile, increases their tolerance to stress and starvation, and improves their longevity (Strilbytska et al. 2022). Because our flash joule-produced graphene is pure graphene without any functionalization, we decided that it would be interesting to investigate the biological impacts of this material.

Almost all organ system of *Drosophila* show similarities with that of humans (Ugur et al. 2016). The central nervous system of *Drosophila* consists of a bilaterally symmetrical brain, neurons, and glial cells. From the brain, the neuronal extensions cover the whole body (Allocca, Zola, and Bellosta, 2018). A longitudinal tube-like heart extends along the abdomen dorsally. These four-chambered heart connected by a valve shows similar physiology to the human heart (Lin et al. 2011). Nutrients and hormones are supplied to internal organs by hemolymph. *Drosophila* and the human intestine are endothelial in origin, including a monolayer of cuboidal epithelial cells, enterocytes, and stem cells. Due to the physiological similarity of *Drosophila* and vertebrate gut, the midgut epithelium of *Drosophila* became a leading platform to study signaling pathways such as EGFR, Notch, Hedgehog, and Wg/Wnt signaling (Apidianakis and Rahme 2011). Analogous to podocytes of glomeruli in the case of the human kidney, fruit fly also has nephrocytes named garland cells in the thorax and pericardial cells in the abdomen, specified for excretion. Considering all these information, we thought this model organism was the best for studying flash joule-synthesized graphene's toxicity and antidiabetic properties.

Characterization of graphene

The physicochemical properties of the synthesized graphene were characterized via several methods. The surface features of the graphene were analyzed using FE-SEM. The obtained image showed wrinkle-shaped and layered sheets of graphene piled upon each other (Fig. 1a). The graphene's HR-TEM image (1b, b') shows a thin single layer under TEM. The graphene was analyzed by X-ray diffraction (XRD). XRD analysis showed a 2θ range of 30.412° and 50.583° corresponding to the presence of calcite and graphene, respectively. Interplanner spacing (d-spacing) for $2\theta = 30.412°$ was 3.379 nm, and d-spacing for $2\theta = 50.583°$ was 2.099 nm. This explains the crystallographic structure of the graphene (Fig. 1c). The UV–vis spectra of graphene exhibit broad absorption feature in the entire UV–vis range, suggesting its suitability as a visible light active material (Fig. 1d). SEM–EDS spectra of graphene show only one peak at carbon, from which we found that our flash joule-synthesized graphene has 100% carbon in it (Fig. 2). Some previous studies about SEM/EDS patterns of graphene derivatives include traditional graphene (C-94.37%, O-4.17%) (Manoj 2015), graphene-oxide (C-57%, O-43%) (Feng et al. 2011), reduced graphene oxide (C-68%, O-28%). In contrast, our flash joule-synthesized graphene has only carbon without any functional group, which explains its purity.

Toxicity assessment using *Drosophila melanogaster*

The 3rd instar larvae were analyzed for the presence of graphene within the gut by employing a Raman spectrometer. Raman spectra were used to recognize the metals and metal oxides. The spectra represented four bands at 1123.65 cm^{-1}, 1349.60 cm^{-1}, 1584.81 cm^{-1}, and 2925.25 cm^{-1}, corresponding to vibration modes of cytochrome C, D band, G band, and 2D band of graphene, respectively Fig. 3 (a'-d'). The intensity ratio of the D and G bands (I_D/I_G) is 0.85. The lower the I_D/I_G ratio, the purer the material is. In that case, our synthesized graphene has an intensity ratio nearly equal to graphene, graphene oxide (GO), HRP-rGO, Fe_3O_4-rGO (magnetic graphene nanocomposite), and GTE-rGO (green synthesized graphene) [Table 1]. A lower (I_D/I_G) ratio indicates that the flash joule-heated graphene is pure. The strong G band denotes optical E_2g vibration in the plane, and the D band indicates disorders due to the A_1g breathing mode of vibrations of graphene. Raman spectroscopic analysis

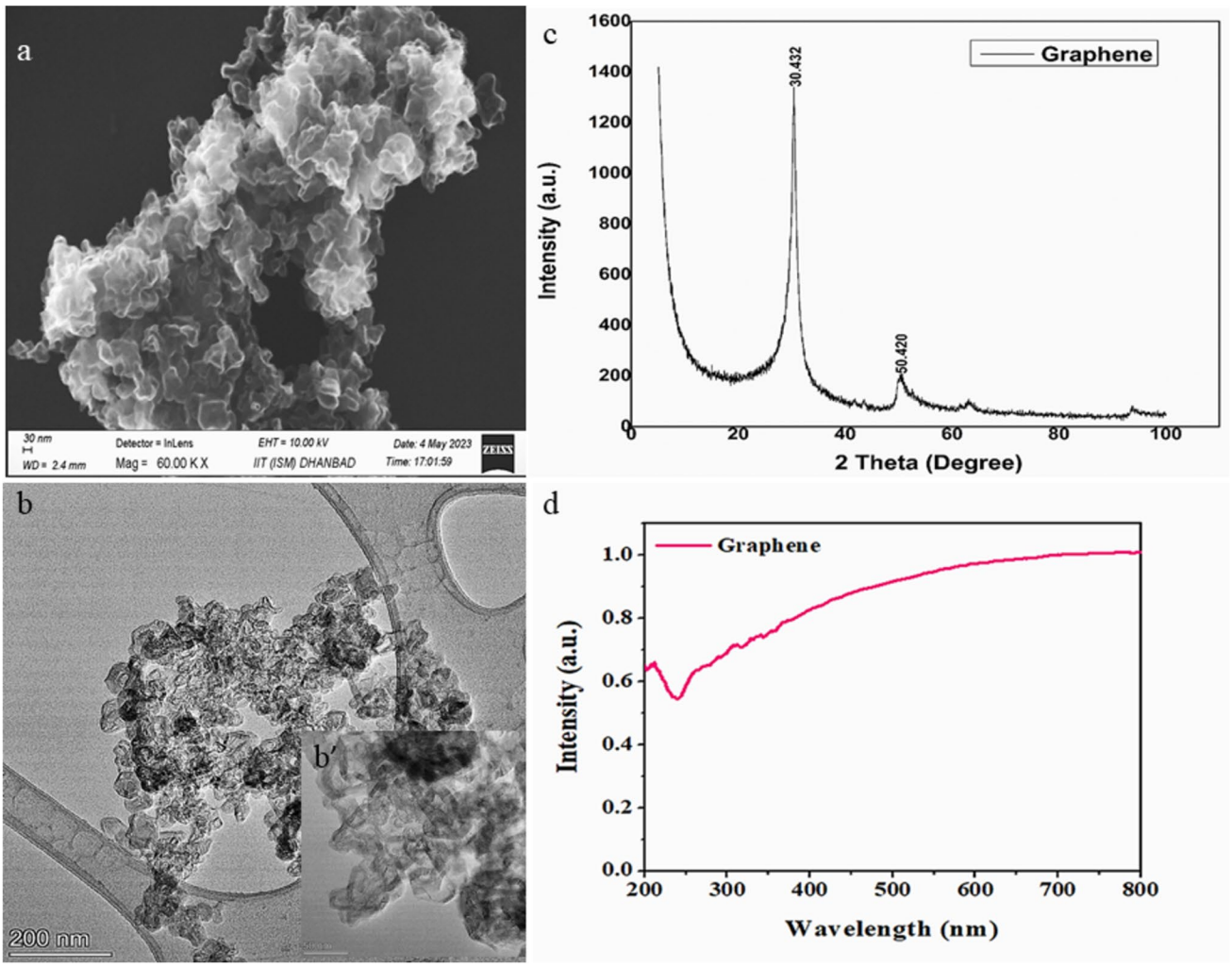

Fig. 1 **a** FE-SEM images of graphene, **b** and **b**' HR-TEM images of graphene, **c** X-ray diffraction analysis of graphene, **d** UV–visible spectra of graphene

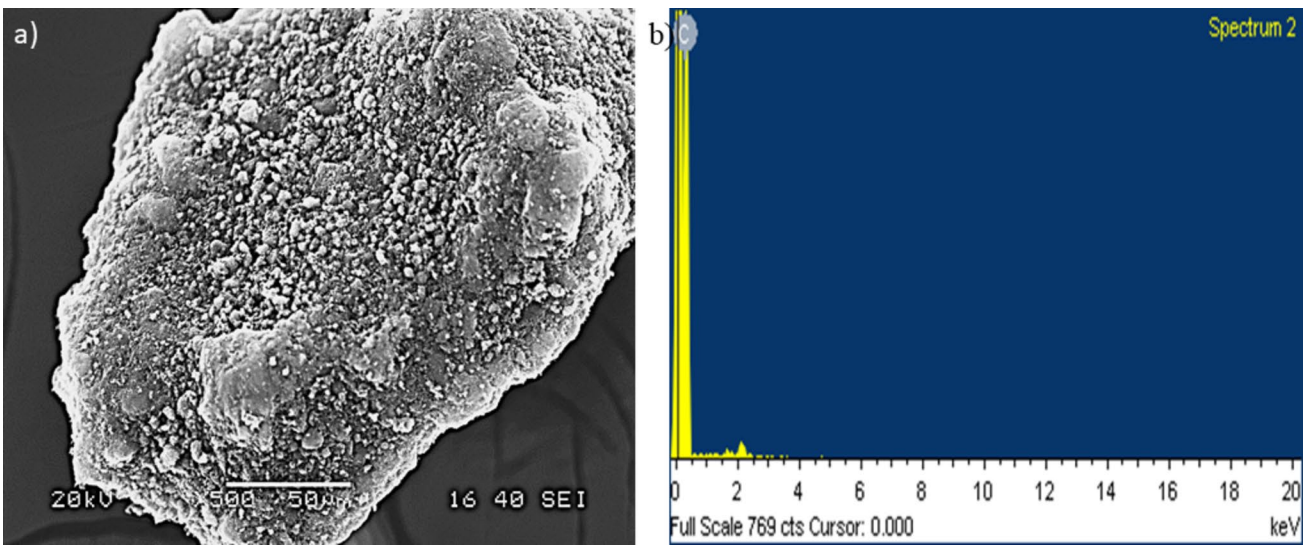

Fig. 2 **a** SEM images of graphene powder, **b** SEM–EDX spectra of graphene

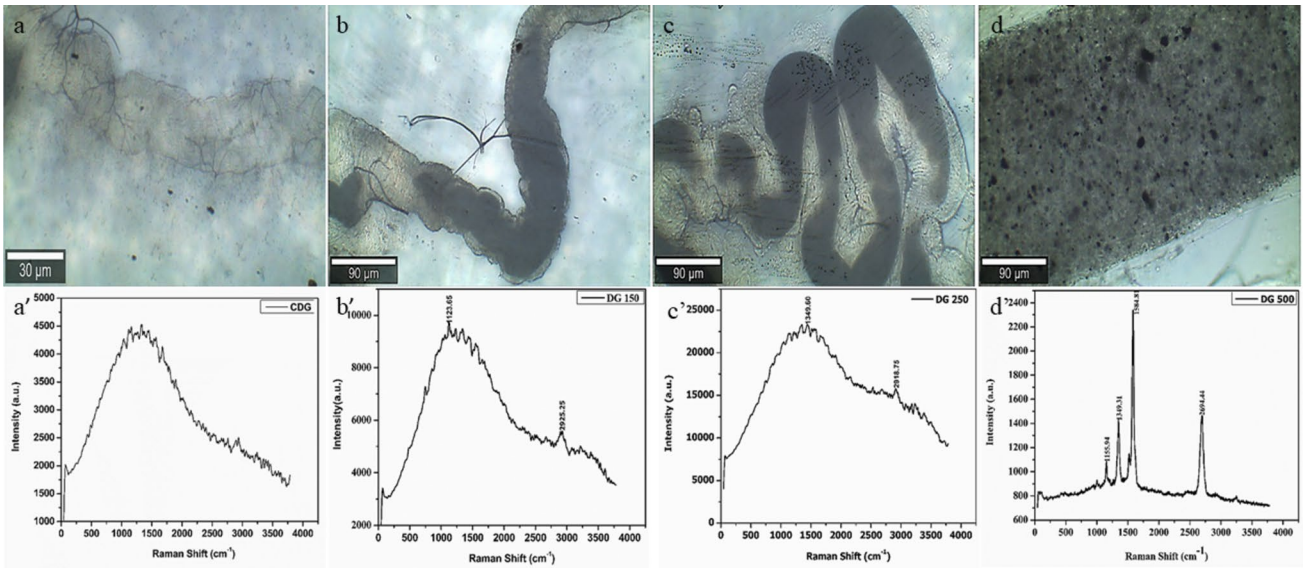

Fig. 3 **a**–**d** Raman spectroscopic images showing the different concentrations of graphene deposition in the gut of graphene-treated flies, **a** control, **b**100 µM graphene, **c** 250 µM graphene, **d** 500 µM graphene, **a**'–**d**' Raman spectroscopic graphene band at different concentrations inside the gut **a**' control, **b**'100 µM graphene, **c**, **a** 250 µM graphene, **d** 500 µM graphene

Table 1 The Raman intensity ratio of different graphene derivatives

Sl. no.	Graphene-based compounds	I_D	I_G	I_D/I_G	References
01	Graphite (grade 3775)	1365 cm^{-1}	2747 cm^{-1}	0.49	(Bokobza et al. 2015)
02	Graphite (grade 4827)	1358 cm^{-1}	2728 cm^{-1}	0.49	(Bokobza et al. 2015)
03	Graphite (grade 4124)	1358 cm^{-1}	2722 cm^{-1}	0.49	(Bokobza et al. 2015)
04	Graphene	1350 cm^{-1}	1580 cm^{-1}	0.85	(Childres et al. 2013)
05	Graphene oxide (GO)	1353 cm^{-1}	1605 cm^{-1}	0.84	(Johra et al. 2014)
06	Reduced GO (rGO)	1326 cm^{-1}	1601 cm^{-1}	1.9	(Behrouzifar et al. 2021)
07	HRP-rGO	1368 cm^{-1}	1619 cm^{-1}	0.84	(Behrouzifar et al. 2021)
08	Fe_3O_4-rGO	1381 cm^{-1}	1580 cm^{-1}	0.76	(Vatandost et al. 2021)
09	GTE-rGO	1350 cm^{-1}	1575 cm^{-1}	0.85	(Vatandost et al. 2020a, b)

confirmed that graphene accumulates in the adult *Drosophila melanogaster* (Fig. 3a-d). Next, we checked whether the accumulated graphene had any toxic effect on the gut. Toxic nanoparticles often lead to nuclear fragmentation, formation of macronuclei, hyperplasia, and alteration in the shape of the nuclei (Mishra, Panda, BARIK, Mondal, and Panda, 2023).

DAPI is a fluorophore that binds both live and fixed cells. After binding (Dmitrieva and Burg 2008), its fluorescence intensity increases up to 20 times, appearing blue under UV light (Lakowicz et al. 1997). Mainly, DAPI binds the AT-rich region of the minor grove of double-stranded DNA (Gryczynski et al. 1996). DAPI (D9542, Sigma-Aldrich, Merck, Germany) stained almost all the nuclei of the control gut sample, as the circular nucleus was visible and appeared blue. However, applying graphene at concentrations of 0.02%, 0.05%, and 0.5% did not result in any observable nuclear damage (Fig. 4a-d), suggesting that the synthesized graphene is non-toxic.

Several neurons coordinate inside the brain to regulate the crawling of larvae. The locomotory behavior of larvae includes twists, turns, linear crawling, burrowing, and other movements. Proper signaling and coordination between muscles, neurons, and the neuromuscular junction is essential for regulated and uniform crawling (Nichols et al. 2012). Any abnormalities in crawling behavior, such as slowed or confused paths, indicate a neuronal disorder (Wang et al. 2002). The larval locomotory behavior can be studied by examining their crawling speed and the trajectory of their crawling path. An irregular and disoriented crawling trajectory can serve as an indicator of neuronal impairment. In contrast, reduced crawling speed may be attributed to obesity, impaired neural communication between neurons and muscles, or diminished muscle strength. However, no

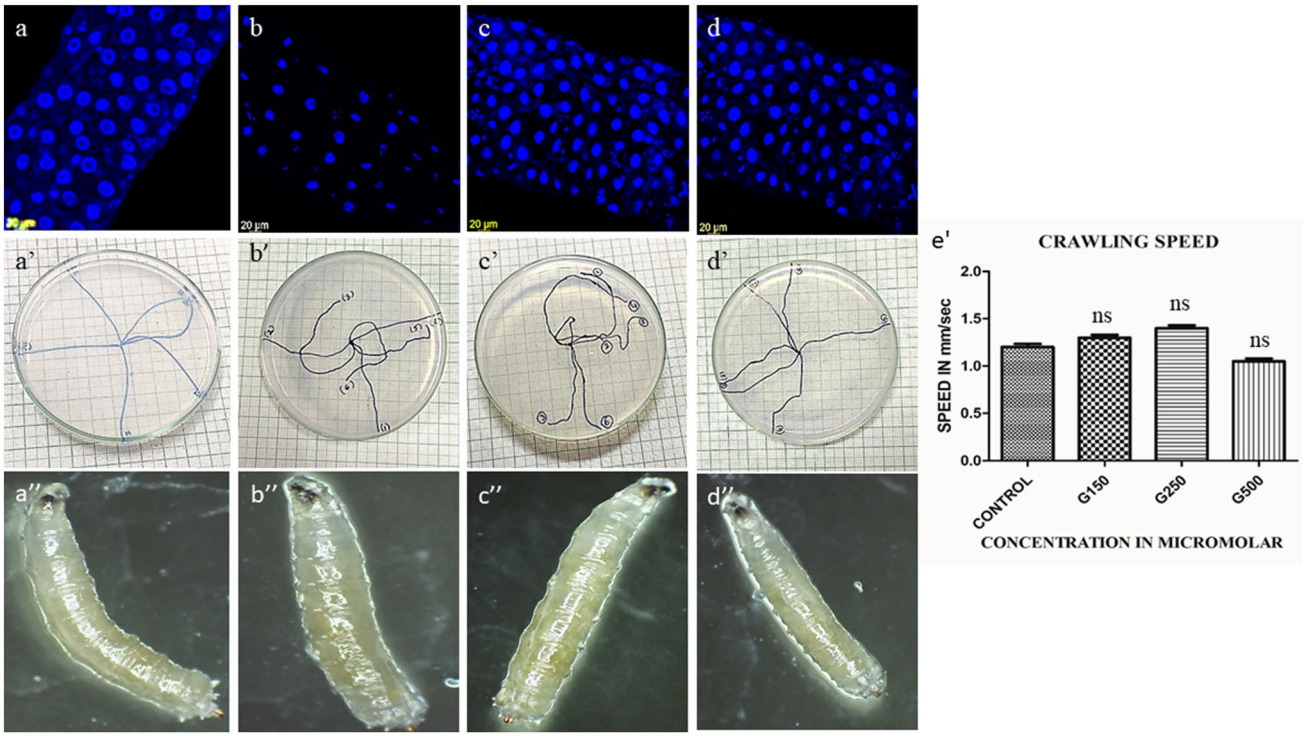

Fig. 4 a–d DAPI staining images showing nuclear arrangements in the gut **a** control, **b** 100 µM graphene, **c** 250 µM graphene, **d** 500 µM graphene, **a**'–**d**' Crawling path of 3rd instar larvae, **a**' control, **b**' 100 µM graphene **c**' 250 µM graphene **d**' 500 µM graphene **e**' Graph showing crawling speed of both control and graphene-treated larvae, **a**''–**d**'' Trypan blue dye exclusion assay of 3rd instar larvae **a**'' control, **b**'' 100 µM graphene, **c**'' 250 µM graphene, **d**'' 500 µM graphene

variation was observed in the crawling path and crawling speed of the larva fed with graphene compared with the control larva. Furthermore, no significant deviations or changes in direction were observed in the trajectory of their crawling movement (Fig. 4a'-d'). The control larva's mean velocity was 1.2 ± 0.06 mm/s. The crawling speed of the graphene-treated larvae was found to be 1.30 ± 0.05 mm/s (P value 0.2560, paired two-tailed t test) at a concentration of 150 µM, 1.40 ± 0.045 mm/s (P value 0.0878 paired two-tailed t test) at 250 µM, and 1.05 ± 0.05 mm/s (P value 0.1125 paired two-tailed t test) at 500 µM (Fig. 3e'). These values were comparable to the crawling speed of the control larvae.

Trypan blue dye exclusion assay is based on the principle that the plasma membrane of the live cell never allows any external dye to pass through it into the cell unless the dye is highly permeable to the plasma membrane. But in a dead cell, the plasma membrane cannot protect the cell, and the dye enters the cell, and that region appears blue. Hence, this assay can be a great approach to distinguishing between live and dead cells (Sabat et al. 2016; Siddique 2012). The integrity and functionality of the gut plasma membrane in larvae treated with graphene were observed to be preserved, as evidenced by the absence of positive results in trypan blue staining. The absence of blue coloration was observed within the internal structure of the larval body (Fig. 4a''-d''). In both control and graphene-fed larvae, the plasma membranes effectively impeded the penetration of the dye into the cell. The findings from these two experiments support the conclusion that ingesting graphene through dietary means does not result in any detrimental effects on the larval gut.

Adult flies naturally climb against gravity. The phenomenon of negative geotaxis behavior, also known as climbing behavior, is an intrinsic characteristic observed in adult *Drosophila* individuals (Li et al. 2020). In the control group, it was observed that an average of $82 \pm 3.6\%$ of the flies successfully ascended to the 10.6 cm mark, which corresponds to 50% of the cylinder's length. In addition, around $57.3 \pm 5.13\%$ of the flies could climb beyond the 16 cm mark, corresponding to 80% of the cylinder's height. The adult flies subjected to graphene treatment exhibited climbing behavior indistinguishable from that of the control group of adult flies. The observed percentages of flies capable of surpassing the 10.6 cm threshold were $80 \pm 4\%$ (p-value 0.6914, paired two-tailed t test) in the 150 µM condition, $80.33 \pm 3.6\%$ (p-value 0.3527, paired two-tailed t test) in the 250 µM condition, and $71.66 \pm 6.80\%$ (p-value 0.1939, paired two-tailed t-test) in the 500 µM condition. In a similar vein, the proportion of flies capable of ascending beyond the 16 cm threshold was observed to be approximately

60.66 ± 5.13% (p-value 0.722, paired two-tailed *t* test) in the presence of a 150-µM concentration, 66.33 ± 4.725% (*p*-value 0.2438, paired two-tailed *t* test) when exposed to a 250-µM concentration, and 54.66 ± 3.5% (*p*-value 0.625, paired two-tailed *t* test) when subjected to a 500-µM concentration of graphene treatment (Fig. 5). Both crawling and climbing assays have demonstrated that graphene is non-neurotoxic.

The approach of forward genetics is based on studying the genetic basis of a specific phenotype. Hence, phenotypic defects can indicate an alteration in gene function or genetic mutation. No phenotypic defects were observed in adult flies treated with graphene. In each experimental configuration, a comprehensive examination was conducted on the phenotypic characteristics of approximately 25 flies, encompassing both males and females. The eye, wing, thorax, and abdomen phenotypes were meticulously scrutinized, and no discernible alterations were observed (Fig. 6).

Antidiabetic property of graphene

Type 2 diabetes (T2D) is often accompanied by a range of pathologies, such as obesity, cardiovascular disease, fatty liver, neuropathy, retinopathy, and nephropathy. Insulin resistance arises from multiple factors, encompassing genetic predisposition, obesity, and dietary patterns. Obesity is widely recognized as a prominent clinical risk factor for Type 2 diabetes (T2D) in the human population. According to a study conducted by Mokdad et al. in 2003, approximately 55% of individuals diagnosed with T2D are classified as obese (Muoio and Newgard 2008). The metabolic regulation observed in *Drosophila* exhibits significant parallels with that of mammals. The genome of the organism in question harbors conserved metabolic regulators, such as SirT, PGC-1α, FOXO, TOR, Akt, and nuclear receptors (Muoio and Newgard 2008). The *Drosophila* insulin-like peptides (DILPs) exhibit sequence, structural, and functional resemblances to insulin-like growth factors and insulin found in vertebrates. These DILPs serve a role in growth and glucose homeostasis regulation. DILPs and the glucagon analog adipokinetic hormone (AKH) regulate glucose levels in insect hemolymph. Fly insulin-producing cells, present inside the median neurosecretory cells, which is homologous to pancreatic β cell, can be eliminated to stimulate type 1 diabetes by increasing hemolymph sugar concentrations (Rulifson et al. 2002). After ablation of the corpora cardiaca, the organ that produces AKH, the quantity of hemolymph glucose is reduced in the case of *Drosophila* (Kim and Rulifson 2004). Previous studies have indicated that including sucrose in a diet at a concentration of up to 1 M leads to diabetes in *Drosophila* (Palanker Musselman et al. 2011). Building upon this established knowledge, we conducted an experiment in which *Drosophila* was fed a diet containing 1 M sucrose to induce diabetes. Subsequently, we looked into the potential antidiabetic properties of graphene in these diabetic flies.

The developmental cycle of adult diabetic flies was examined in a graphene medium for 7 days. *Drosophila* possesses the holometabolous type of development, which is around 10 days. About 24 h after the fertilization event, the egg hatches into larvae, which undergo three molts that take approximately 5.5–6 days, and after that, they experience a metabolically quiescent pupa phase. The pupa undergoes a complete metamorphosis for 3.5–4.5 days and finally hatches into an adult at about 10.5 days. Growth and development depend on diet. Diet changes can delay development and may cause death at any developmental stage. The high-sugar diet (HSD) food medium delayed the 2nd-to-3rd instar transition. In the HSD medium, 3rd instar larvae emerged after 7.5 days, i.e., 180 h, delaying the arrival of the first adult up to 12 days. The graphene medium had an unanticipated influence on

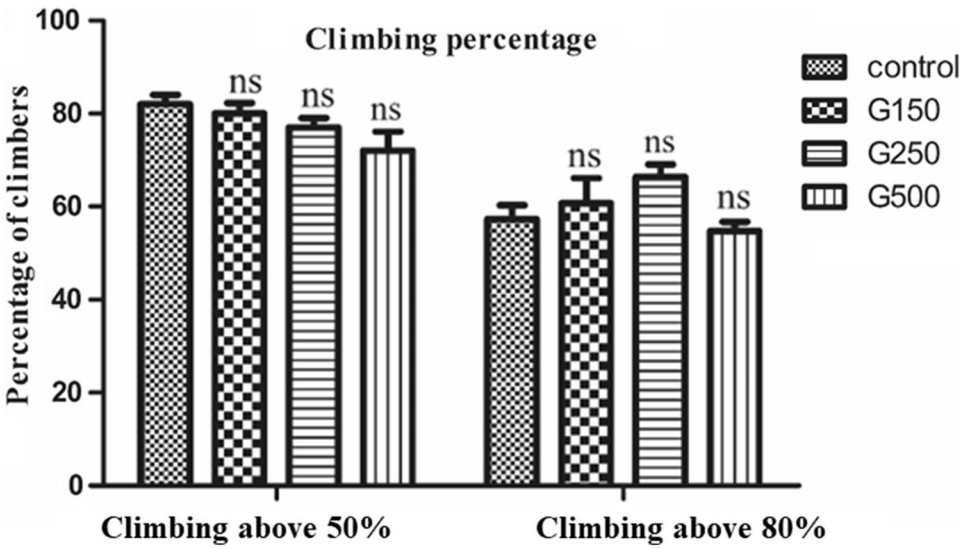

Fig. 5 Graph showing the percentage of flies from both control and experimental setups able to climb above 50% and 80% of the length of the glass cylinder at a time interval of 10 s

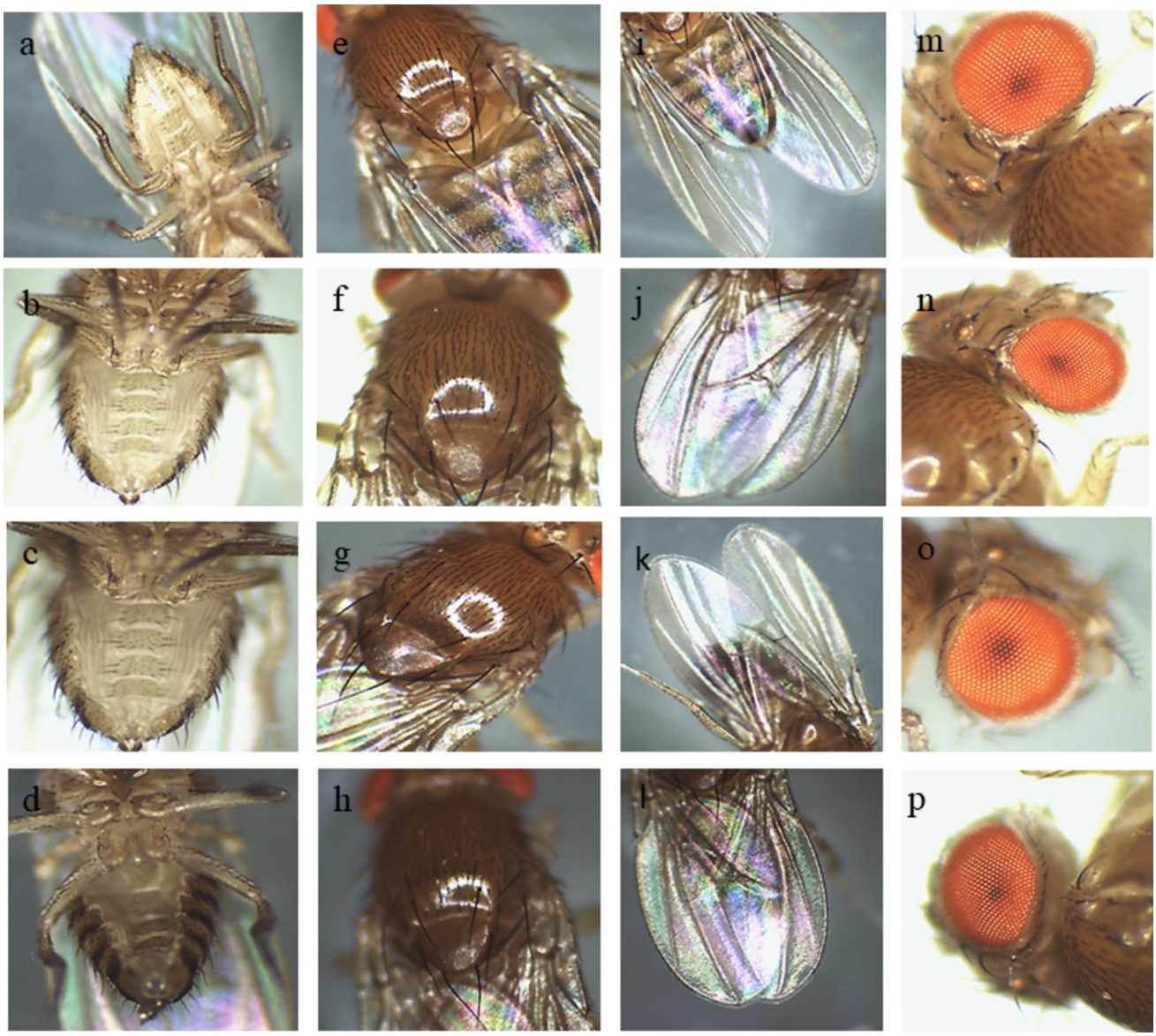

Fig. 6 Adult phenotype, **a–d** abdomen phenotype at different concentrations, **e–h** thorax phenotype at different concentrations, **i–l** wing phenotype at different concentrations, **m–p** eye phenotype at different concentrations

early development. Specifically, it takes larvae to reach the 3rd instar stage in 5 days (120 h) and expedites the first adult's emergence to 10 days (Fig. 7a).

Newly emerging pupae were counted every 6 h for 72 h. A graph was plotted for the pupal count of each experimental setup (Fig. 7b). The graph suggests evidence that graphene present in food induces early development.

An enzymatic assay using glucose oxidase/peroxidase reagent was done to estimate the free glucose amount (Tennessen et al. 2014). Adult control flies had a free glucose concentration of 0.279 ± 0.016 µg/ml, whereas diabetic flies of the same age had a circulating sugar level that was two-fold higher, 0.623 ± 0.017 µg/ml. This value decreases as the concentration of graphene increases, from 0.631 ± 0.019 µg/ml (P value 0.024, paired two-tailed *t* test, with that of HSD flies' hemolymph glucose level) at G150 µm to 0.483 ± 0.02 µg/ml (P value 0.0065, paired two-tailed *t* test, with that of HSD flies' hemolymph glucose level) at G250µm, 0.375 ± 0.018 µg/ml (P value < 0.001 paired two-tailed *t* test, with that of HSD flies' hemolymph glucose level) at G500 µm. At the same time, changing diet to a standard food medium from a high-sugar medium could not significantly alter this value. The free glucose concentration remained at 0.596 ± 0.019 µg/ml (P value 0.106, paired two-tailed *t* test, with that of HSD flies' hemolymph glucose) (Fig. 8a).

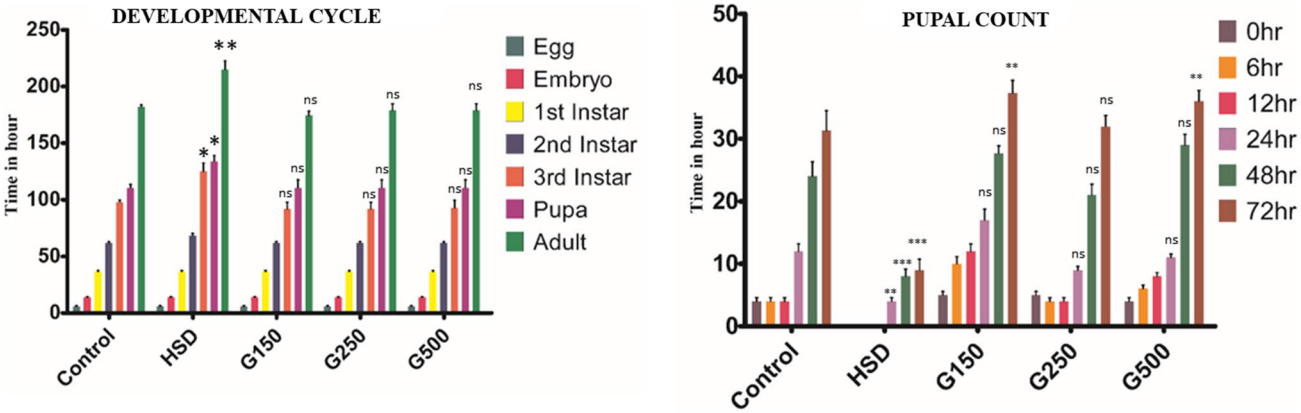

Fig. 7 **a** Graph showing the developmental cycle of flies at different concentrations, x-axis showing different concentrations, y-axis showing time in hours, **b** Graph showing the number of pupa in different time intervals at different concentrations, x-axis showing different concentrations, y-axis showing the number of pupa

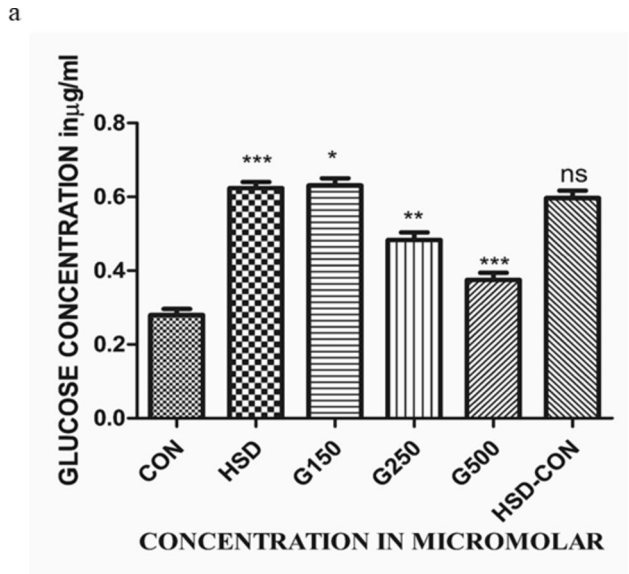

Fig. 8 **a** Graph showing adult flies' hemolymph glucose levels in different food mediums

Obesity is the primary symptom of diabetes, and the accumulation of fat in the form of lipid droplets causes obesity and weight gain. A fluorescence-based approach was used to detect the amount of lipid droplet accumulation and the effect of graphene treatment on fatty flies. Histological staining of adult *Drosophila* gut was done using a hydrophobic dye 9-diethylamino-5H-benzo[a]phenoxazine-5-one (Nile red) (Ray et al. 2019). The fluorescence property of the dye is quenched after exposure to water or hydrophilic solvent, while the intensity increases when it reacts with organic solvents or lipid droplets (Rumin et al. 2015). Due to its pronounced hydrophobic properties, Nile red dye readily penetrates the cellular membrane and selectively associates with lipid droplets, resulting in a distinctive red coloration that mirrors the morphology of the lipid droplet (Greenspan et al. 1985). Therefore, Nile red staining provides insights into lipid droplets' presence, shape, size, and quantity. Consuming high-caloric content leads to an elevation in lipid levels within the body. The accumulation of lipids and fat exhibits variability concerning the specific physiological condition experienced by an individual's body. Undoubtedly, including a high-sucrose content in a diet of up to 35% will substantially increase lipid accumulation. However, following the application of graphene treatment, there was a remarkable reduction in the size and abundance of lipid droplets, which was observed to be directly proportional to the concentration of graphene. Merely altering the fly's diet to conventional food was insufficient to mitigate lipid accumulation satisfactorily (Fig. 9).

Several endogenous and exogenous factors, such as disease conditions, including diabetes, microbial infection, environmental stress, and ingestion of toxic chemicals in food, disturb the body's antioxidant defense mechanism. Due to the disability of the antioxidant defense mechanism, the production of reactive oxygen species (ROS) exceeds the degradation of ROS (Zorov et al. 2014). To detect the amount of ROS production in diabetic flies and to confirm whether graphene treatment decreases the ROS amount, we performed histological staining of DCFH-DA. The cellular reactive oxygen species (ROS) induce an oxidation reaction of the DCFH-DA dye, enhancing the green fluorescence intensity observed in gut samples through confocal microscopic imaging. The fluorescence-based method of detecting ROS is based on the principle that when the dye DCFH-DA enters the body, it gets hydrolyzed by several esterases and converted into a non-fluorescent $DCFH^{-}$ which, after diffusing into a cell, gets oxidized with several ROS such as H_2O_2, NO_2, and O_2^{-} and gets converted to a green fluorescent DCF

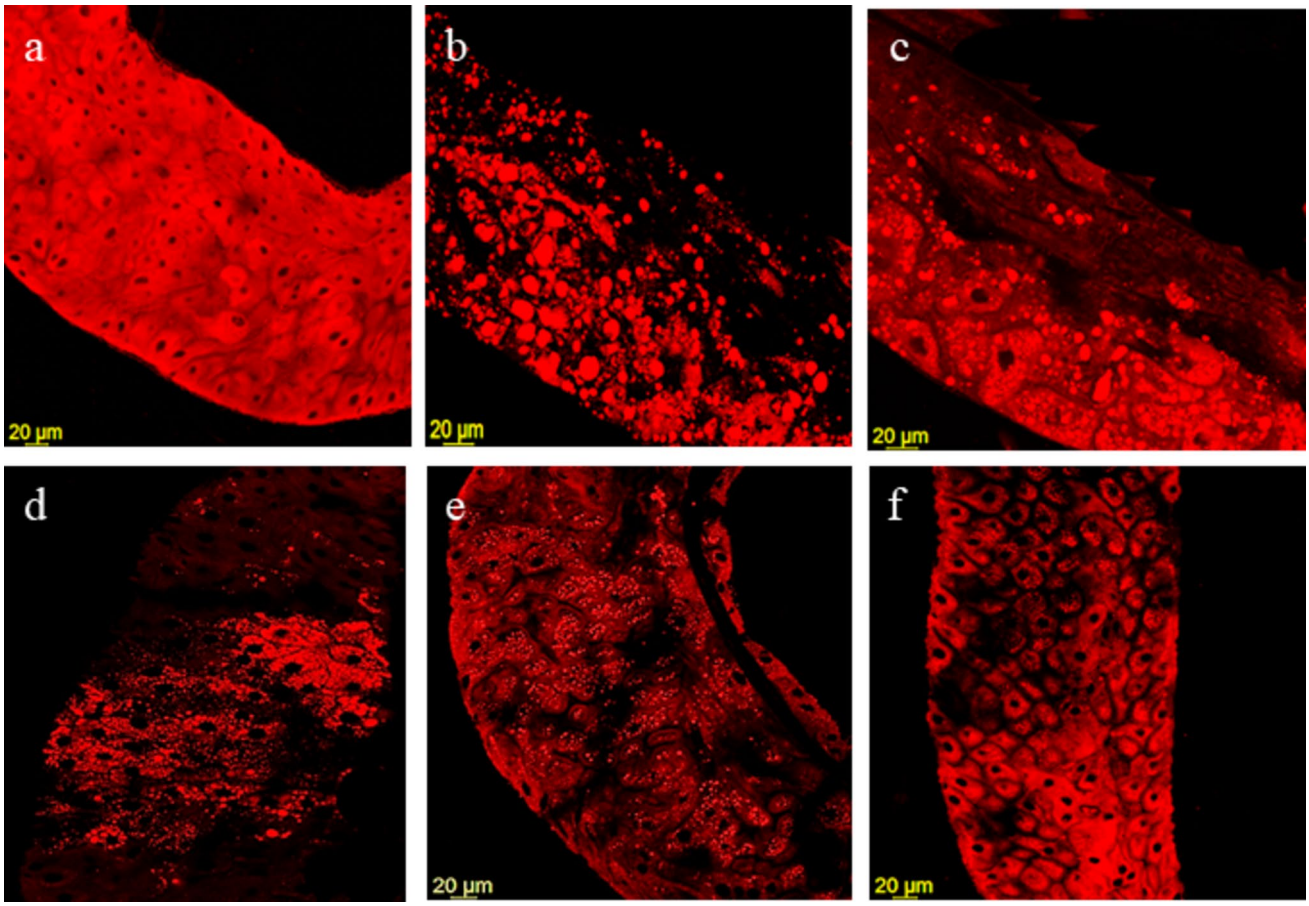

Fig. 9 Nile red staining images **a** control, **b** HSD flies, **c** Diabetic flies transferred to control food for 7 days, **d**–**f** Diabetic flies transferred to graphene-containing food, **d** 100 µM, **e** 250 µM, **f** 500 µM

probe (Royall and Ischiropoulos 1993). The intensity of green fluorescence indicates the amount of ROS. The fluorescence intensity of diabetic flies was found to be reduced after graphene treatment. Remarkably, the flies that underwent graphene treatment exhibited noteworthy outcomes. The average fluorescence intensity of produced ROS in the case of control flies was 6.672 ± 0.099, and for diabetic flies, it was 13.04 ± 0.3915 graphene treatment, the fluorescence intensity was reduced significantly to 8.5 ± 0.472 (p-value 0.0021, paired two-tailed t test) for 150 µM, 7.43 ± 0.378 (p-value 0.0033, paired two-tailed t test) for 250 µM, and 6.06 ± 0.152 (p-value 0.0007, paired two-tailed t test) for 500 µM, which is 57% less than that of the HSD flies. But when the HSD flies were subjected to a control diet for 7 days, the fluorescence intensity was decreased to 9.553 ± 0.391 (p-value 0.0035, paired two-tailed t test). The observed substantial decrease in fluorescence intensity after graphene treatment provides compelling evidence of its efficacy as a potent inhibitor of several physiological complications associated with diabetes, possibly due to reactive oxygen species (ROS) accumulation (Fig. 10).

Antibacterial activity of graphene

Unregulated hyperglycemia impairs innate and adaptive immune mechanisms, making the body susceptible to microorganisms. Diabetes can also cause chronic consequences such as neuropathy (sensorimotor and autonomic) and peripheral vascular disease, which lead to skin ulcers and secondary bacterial infections, which further increase infection-related mortality in diabetes. Periodontitis is caused by *Staphylococcus, Streptococcus,* and *Bacillus* species of bacteria (Ali et al. 2021; Wang et al. 2009), and malignant otitis externa from *Pseudomonas aeruginosa* is linked to diabetes (Carlton et al. 2018; Yang et al. 2020). Emphysematous cholecystitis is caused by *Clostridium perfringens* and *Escherichia coli* (Nagendra et al. 2022; Safwan and Penny 2016). Depending on location and severity, empirical and culture-specific antibiotic regimens are recommended for different bacterial infections. This study reveals graphene's potential antibacterial action to eliminate germs and reduce diabetes-related bacterial infections. From Graph 11, it was confirmed that graphene shows antibacterial properties

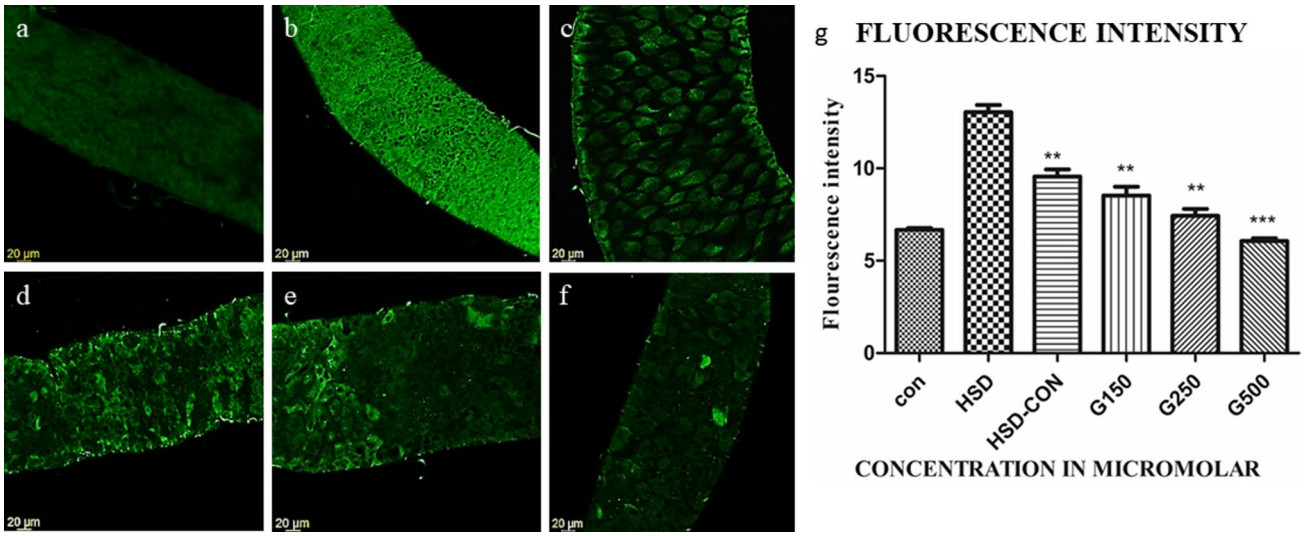

Fig. 10 DCFH-DA staining images **a** control, **b** HSD flies, **c** Diabetic flies transferred to control food for 7 days, **d**–**f** Diabetic flies transferred to graphene-containing food, **d** 100 µM, **e** 250 µM, **f** 500µ **g** Graph showing fluorescence intensity of ROS

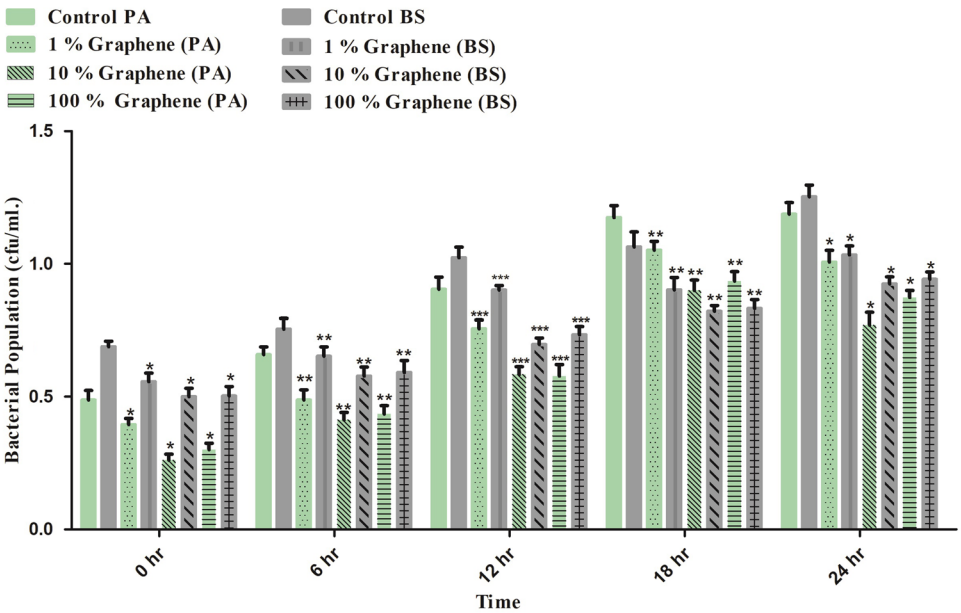

Fig. 11 Graph showing antibacterial properties of graphene

against the bacteria mentioned above at 1% and 10% concentrations. However, 100% graphene does not show satisfactory results as it is agglomerated at the bottom of the well (see Fig. 11).

Conclusion

This study presents the novel application of pure graphene, devoid of any functional groups, as a therapeutic compound that can be administered through dietary means. The findings demonstrate its potential as an antidiabetic agent and its ability to promote early development while exhibiting a favorable non-toxic profile. A notable reduction in circulating sugar and lipid deposition levels and accelerated growth were observed upon treatment with graphene at concentrations ranging from 0.02% to 0.5%. Furthermore, a notable reduction in the magnitude of reactive oxygen species, which exhibited elevated levels in individuals with diabetes, is also observed. Graphene has a favorable and inducible property on growth and development. Based on the aforementioned findings and the non-toxic nature of graphene, it can be

inferred that applying graphene at a concentration range of 0.02–0.5% reduces symptoms resembling those of diabetes.

Future prospective

In the invertebrate model, the flash joule-produced graphene is investigated as an antidiabetic agent with no discernible adverse effects. Subsequent investigations could examine graphene's antidiabetic characteristics in vertebrate model species. Our future research will also include determining graphene's function on the insulin signaling pathway and the antioxidant defense mechanism at a molecular level. There are more physiological consequences of diabetes. Future research will also examine graphene's potential for treating physiological implications of diabetes, such as diabetic nephropathy, neuropathy, and retinopathy.

Acknowledgements We thank Shri Narayan Agnihotri, Director of Graphenera Carbon Private Limited, for providing synthesized graphene free of cost. KD is thankful to UGC for financial support (211610018329). DP is grateful to MHRD for financial aid. We thank NIT Rourkela for the equipment and facilities used in this study.

Declarations

Conflict of interest There is no conflict of interest.

Ethical approval The experiments are complied with ethical standard.

References

Abbas Q, Shinde PA, Abdelkareem MA, Alami AH, Mirzaeian M, Yadav A, Olabi AG (2022) Graphene synthesis techniques and environmental applications. Materials 15(21):7804

Abdi R, Ghorbani-HasanSaraei A, Raeisi SN, Karimi F (2020) A gallic acid food electrochemical sensor based on amplification of paste electrode by Cdo/CNTs nanocomposite and ionic liquid. J Med Chem Sci 3(4):338–344

Ali T, Rumnaz A, Urmi UL, Nahar S, Rana M, Sultana F, Islam S (2021) Type-2 diabetes mellitus individuals carry different periodontal bacteria. Pesqui Bras Em Odontopediatr e Clín Integr. https://doi.org/10.1590/pboci.2021.049

Allocca M, Zola S, Bellosta P (2018) The fruit fly, *Drosophila melanogaster*: modeling of human diseases (Part II). *Drosophila melanogaster*-model for recent advances in genetics and therapeutics. InTech, New York, pp 131–156

Apidianakis Y, Rahme LG (2011) Drosophila melanogaster as a model for human intestinal infection and pathology. Dis Model Mech 4(1):21–30

Behrouzifar F, Shahidi S-A, Chekin F, Hosseini S, Ghorbani-Hasan-Saraei A (2021) Colorimetric assay based on horseradish peroxidase/reduced graphene oxide hybrid for sensitive detection of hydrogen peroxide in beverages. Spectrochim Acta Part A Mol Biomol Spectrosc 257:119761

Bokobza L, Bruneel J-L, Couzi M (2015) Raman spectra of carbon-based materials (from graphite to carbon black) and of some silicone composites. C 1(1):77–94

Carlton DA, Perez EE, Smouha EE (2018) Malignant external otitis: the shifting treatment paradigm. Am J Otolaryngol 39(1):41–45

Cartamil-Bueno SJ, Cavalieri M, Wang R, Houri S, Hofmann S, van der Zant HS (2017) Mechanical characterization and cleaning of CVD single-layer h-BN resonators. Npj 2D Mater Appl. 1(1):16

Chandu B, Mosali VSS, Mullamuri B, Bollikolla HB (2017) A facile green reduction of graphene oxide using Annona squamosa leaf extract. Carbon Lett 21:74–80

Chekin F, Teodorescu F, Coffinier Y, Pan G-H, Barras A, Boukherroub R, Szunerits S (2016) MoS2/reduced graphene oxide as active hybrid material for the electrochemical detection of folic acid in human serum. Biosens Bioelectron 85:807–813

Chen Y, Vedala H, Kotchey GP, Audfray A, Cecioni S, Imberty A, Star A (2012) Electronic detection of lectins using carbohydrate-functionalized nanostructures: graphene versus carbon nanotubes. ACS Nano 6(1):760–770

Childres I, Jauregui LA, Park W, Cao H, Chen YP (2013) Raman spectroscopy of graphene and related materials. New Dev Photon Mater Res 1:1–20

De Lázaro I, Vranic S, Marson D, Rodrigues AF, Buggio M, Esteban-Arranz A, Kostarelos K (2019) Graphene oxide as a 2D platform for complexation and intracellular delivery of siRNA. Nanoscale 11(29):13863–13877

Dmitrieva NI, Burg MB (2008) Analysis of DNA breaks, DNA damage response, and apoptosis produced by high NaCl. Am J Physiol-Renal Physiol 295(6):F1678–F1688

Dong G, Zhang Y, Pan Q, Qiu J (2014) A fantastic graphitic carbon nitride (gC 3N 4) material: electronic structure, photocatalytic and photoelectronic properties. J Photochem Photobiol C Photochem Rev 20:33–50

Elias DC, Nair RR, Mohiuddin T, Morozov S, Blake P, Halsall M, Geim A (2009) Control of graphene's properties by reversible hydrogenation: evidence for graphene. Science 323(5914):610–613

Feng L, Gao G, Huang P, Wang X, Zhang C, Zhang J, Cui D (2011) Preparation of Pt Ag alloy nanoisland/graphene hybrid composites and its high stability and catalytic activity in methanol electro-oxidation. Nanoscale Res Lett 6:1–10

Greenspan P, Mayer EP, Fowler SD (1985) Nile red: a selective fluorescent stain for intracellular lipid droplets. J Cell Biol 100(3):965–973

Gryczynski I, Malak H, Lakowicz JR (1996) Multiphoton excitation of the DNA stains DAPI and Hoechst. Bioimaging 4(3):138–148

Guo Q, Yang Y, Zhao L, Chen J, Duan G, Yang Z, Zhou R (2022) Graphene oxide toxicity in W1118 flies. Sci Total Environ 805:150302

He Y, Wang Z-G, Tang H-W, Pang D-W (2011) Low background signal platform for the detection of ATP: when a molecular aptamer beacon meets graphene oxide. Biosens Bioelectron 29(1):76–81

Huang WT, Shi Y, Xie WY, Luo HQ, Li NB (2011) A reversible fluorescence nanoswitch based on bifunctional reduced graphene oxide: use for detection of Hg 2+ and molecular logic gate operation. Chem Commun 47(27):7800–7802

Hughes ZE, Walsh TR (2015) Computational chemistry for graphene-based energy applications: progress and challenges. Nanoscale 7(16):6883–6908

Jiang J-W, Park HS (2014) Mechanical properties of single-layer black phosphorus. J Phys D Appl Phys 47(38):385304

Johra FT, Lee J-W, Jung W-G (2014) Facile and safe graphene preparation on solution based platform. J Ind Eng Chem 20(5):2883–2887

Kaczmarek-Szczepańska B, Michalska-Sionkowska M, Binkowski P, Lukaszewicz JP, Kamedulski P (2023) 3D-structured and blood-contact-safe graphene materials. Int J Mol Sci 24(4):3576

Kamedulski P, Lukaszewicz JP, Witczak L, Szroeder P, Ziolkowski P (2021) The importance of structural factors for the electrochemical performance of graphene/carbon nanotube/melamine powders

towards the catalytic activity of oxygen reduction reaction. Materials 14(9):2448
Karimi-Maleh H, Karimi F, Fu L, Sanati AL, Alizadeh M, Karaman C, Orooji Y (2022) Cyanazine herbicide monitoring as a hazardous substance by a DNA nanostructure biosensor. J Hazard Mater 423:127058
Kim SK, Rulifson EJ (2004) Conserved mechanisms of glucose sensing and regulation by Drosophila corpora cardiaca cells. Nature 431(7006):316–320
Kumar R, Bauri S, Sahu S, Chauhan S, Dholpuria S, Ruokolainen J, Gupta PK (2023) In vivo toxicological analysis of MnFe2O4@ poly (t BGE-alt-PA) composite as a hybrid nanomaterial for possible biomedical use. ACS Appl Bio Mater 6(3):1122–1132
Lakowicz JR, Gryczynski I, Malak H, Schrader M, Engelhardt P, Kano H, Hell SW (1997) Time-resolved fluorescence spectroscopy and imaging of DNA labeled with DAPI and Hoechst 33342 using three-photon excitation. Biophys J 72(2):567–578
Li X, Zhu H (2015) Two-dimensional MoS2: properties, preparation, and applications. J Materiomics 1(1):33–44
Li QF, Wang H, Zheng L, Yang F, Li HZ, Li JX, Liu Y (2020) Effects of modest hypoxia and exercise on cardiac function, sleep-activity, negative geotaxis behavior of aged female Drosophila. Front Physiol 10:1610
Liao L, Peng H, Liu Z (2014) Chemistry makes graphene beyond graphene. J Am Chem Soc 136(35):12194–12200
Lin N, Badie N, Yu L, Abraham D, Cheng H, Bursac N, Wolf MJ (2011) A method to measure myocardial calcium handling in adult Drosophila. Circ Res 108(11):1306–1315
Liu M, Zhao H, Chen S, Yu H, Zhang Y, Quan X (2011) Label-free fluorescent detection of Cu (II) ions based on DNA cleavage-dependent graphene-quenched DNAzymes. Chem Commun 47(27):7749–7751
Luong DX, Bets KV, Algozeeb WA, Stanford MG, Kittrell C, Chen W, Advincula PA (2020) Gram-scale bottom-up flash graphene synthesis. Nature 577(7792):647–651
Manoj B (2015) Synthesis and characterization of porous, mixed phase, wrinkled, few layer graphene like nanocarbon from charcoal. Russ J Phys Chem A 89:2438–2442
Mishra M (2020) Fundamental approaches to screen abnormalities in Drosophila. Springer, New York
Mishra M, Panda P, Barik BK, Mondal A, Panda M (2023) Drosophila melanogaster as an indispensable model to decipher the mode of action of neurotoxic compounds. Biocell 47(1):51–69
Mohanty N, Berry V (2008) Graphene-based single-bacterium resolution biodevice and DNA transistor: interfacing graphene derivatives with nanoscale and microscale biocomponents. Nano Lett 8(12):4469–4476
Mukherjee S, Nayak N, Mohapatra S, Sahoo JK, Sahoo H, Mishra M (2022) Strontium ferrite as a nontoxic nanomaterial to improve metabolism in a diabetic model of *Drosophila melanogaster*. Mater Chem Phys 281:125906
Muoio DM, Newgard CB (2008) Molecular and metabolic mechanisms of insulin resistance and β-cell failure in type 2 diabetes. Nat Rev Mol Cell Biol 9(3):193–205
Murmu N, Dash K, Panda J, Sahoo G, Sahoo H, Mishra M, Sahu SN (2023) A biscoumarinyl hydrazone based nontoxic fluorescent dye for direct binding and imaging of actin in living cells and organism. Sensors and Actuators b: Chem 399:134741
Nagendra L, Boro H, Mannar V (2022) Bacterial infections in diabetes. Endotext [Internet].
Nair RR, Ren W, Jalil R, Riaz I, Kravets VG, Britnell L, Yuan S (2010) Fluorographene: a two-dimensional counterpart of Teflon. Small 6(24):2877–2884
Nayak N, Mishra M (2021) High fat diet induced abnormalities in metabolism, growth, behavior, and circadian clock in *Drosophila melanogaster*. Life Sci 281:119758
Nayak P, Bag J, Padhan SK, Sahoo H, Sahu SN, Mishra M (2023) Coumarin-based noncytotoxicity fluorescent dye for tracking actin protein in in-vivo imaging. Chem Res Toxicol. https://doi.org/10.1021/acs.chemrestox.3c00051
Ni Z, Liu Q, Tang K, Zheng J, Zhou J, Qin R, Lu J (2012) Tunable bandgap in silicene and germanene. Nano Lett 12(1):113–118
Nichols CD, Becnel J, Pandey UB (2012) Methods to assay Drosophila behavior. J vis Exp 61:e3795
Novoselov KS, Jiang D, Schedin F, Booth T, Khotkevich V, Morozov S, Geim AK (2005) Two-dimensional atomic crystals. Proc Natl Acad Sci 102(30):10451–10453
Ohno Y, Maehashi K, Matsumoto K (2010) Label-free biosensors based on aptamer-modified graphene field-effect transistors. J Am Chem Soc 132(51):18012–18013
Palanker Musselman L, Fink JL, Narzinski K, Ramachandran PV, Sukumar Hathiramani S, Cagan RL, Baranski TJ (2011) A high-sugar diet produces obesity and insulin resistance in wild-type Drosophila. Dis Model Mech 4(6):842–849
Park SY, Park J, Sim SH, Sung MG, Kim KS, Hong BH, Hong S (2011) Enhanced differentiation of human neural stem cells into neurons on graphene. Adv Mater 23(36):H263–H267
Peng Y, Wang Z, Zou K (2015) Friction and wear properties of different types of graphene nanosheets as effective solid lubricants. Langmuir 31(28):7782–7791
Priyadarsini S, Sahoo SK, Sahu S, Mukherjee S, Hota G, Mishra M (2019) Oral administration of graphene oxide nano-sheets induces oxidative stress, genotoxicity, and behavioral teratogenicity in Drosophila melanogaster. Environ Sci Pollut Res 26(19):19560–19574
Pu Y, Zhu Z, Han D, Liu H, Liu J, Liao J, Tan W (2011) Insulin-binding aptamer-conjugated graphene oxide for insulin detection. Analyst 136(20):4138–4140
Ray A, Das S, Chattopadhyay N (2019) Aggregation of Nile red in water: prevention through encapsulation in β-cyclodextrin. ACS Omega 4(1):15–24
Rouway M, Nachtane M, Tarfaoui M, Chakhchaoui N, Omari LEH, Fraija F, Cherkaoui O (2021) Mechanical properties of a biocomposite based on carbon nanotube and graphene nanoplatelet reinforced polymers: analytical and numerical study. J Compos Sc 5(9):234
Royall JA, Ischiropoulos H (1993) Evaluation of 2′, 7′-dichlorofluorescin and dihydrorhodamine 123 as fluorescent probes for intracellular H2O2 in cultured endothelial cells. Arch Biochem Biophys 302(2):348–355
Rulifson EJ, Kim SK, Nusse R (2002) Ablation of insulin-producing neurons in flies: growth and diabetic phenotypes. Science 296(5570):1118–1120
Rumin J, Bonnefond H, Saint-Jean B, Rouxel C, Sciandra A, Bernard O, Bougaran G (2015) The use of fluorescent Nile red and BODIPY for lipid measurement in microalgae. Biotechnol Biofuels 8(1):1–16
Sabat D, Patnaik A, Ekka B, Dash P, Mishra M (2016) Investigation of titania nanoparticles on behaviour and mechanosensory organ of *Drosophila melanogaster*. Physiol Behav 167:76–85
Safwan M, Penny SM (2016) Emphysematous cholecystitis: a deadly twist to a common disease. J Diagn Med Sonogr 32(3):131–137
Salimbahrami SN, Ghorbani-HasanSaraei A, Tahermansouri H, Shahidi S-A (2023) Synthesis, optimization via response surface methodology, and structural properties of carboxymethylcellulose/curcumin/graphene oxide biocomposite films/coatings for the shelf-life extension of shrimp. Int J Biol Macromol 253:126724
Seyedi S, Shahidi S, Chekin F, Ghorbani-HasanSaraei A, Limooei M (2023) Magnetite nanoparticles decorated porous reduced graphene oxide for bio-and medical application. Russ Chem Bull 72(9):2060–2069

Sharif Nasirian V, Shahidi SA, Tahermansouri H, Chekin F (2021) Application of graphene oxide in the adsorption and extraction of bioactive compounds from lemon peel. Food Sci Nutr 9(7):3852–3862

Sheng L, Ren J, Miao Y, Wang J, Wang E (2011) PVP-coated graphene oxide for selective determination of ochratoxin A via quenching fluorescence of free aptamer. Biosens Bioelectron 26(8):3494–3499

Siddique YH (2012) Protective role of curcumin against the toxic effects of cyclophosphamide in the third instar larvae of transgenic Drosophila melanogaster (hsp70-lacZ) Bg9. Altern Med Stud 2(1):e2–e2

Strilbytska O, Semaniuk U, Burdyliuk N, Lushchak O (2022) Evaluation of biological effects of graphene oxide using Drosophila. Phys Chem Solid State 23(2):242–248

Tabrizi M, Shahidi S-A, Chekin F, Ghorbani-HasanSaraei A, Raeisi SN (2022) Reduce graphene oxide/Fe 3 O 4 nanocomposite biosynthesized by sour lemon peel; using as electro-catalyst for fabrication of vanillin electrochemical sensor in food products analysis and anticancer activity. Topics Catal 65:726–732

Tennessen JM, Barry WE, Cox J, Thummel CS (2014) Methods for studying metabolism in Drosophila. Methods 68(1):105–115

Tiwari SK, Kumar V, Huczko A, Oraon R, Adhikari AD, Nayak G (2016) Magical allotropes of carbon: prospects and applications. Crit Rev Solid State Mater Sci 41(4):257–317

Tiwari SK, Mishra RK, Ha SK, Huczko A (2018) Evolution of graphene oxide and graphene: from imagination to industrialization. ChemNanoMat 4(7):598–620

Ugur B, Chen K, Bellen HJ (2016) Drosophila tools and assays for the study of human diseases. Dis Model Mech 9(3):235–244

Vatandost E, Ghorbani-HasanSaraei A, Chekin F, Raeisi SN, Shahidi S-A (2020a) Green tea extract assisted green synthesis of reduced graphene oxide: application for highly sensitive electrochemical detection of sunset yellow in food products. Food Chemistry: X 6:100085

Vatandost E, Saraei AGH, Chekin F, Raeisi SN, Shahidi SA (2020b) Antioxidant, antibacterial and anticancer performance of reduced graphene oxide prepared via green tea extract assisted biosynthesis. ChemistrySelect 5(33):10401–10406

Vatandost E, Ghorbani-Hasan Saraei A, Chekin F, Raeisi SN, Shahidi S-A (2021) Electrochemical sensor based on magnetic Fe3O4–reduced graphene oxide hybrid for sensitive detection of binaphthol. Russ J Electrochem 57(5):490–498

Wang JW, Soll DR, Wu C-F (2002) Morphometric description of the wandering behavior in Drosophila larvae: a phenotypic analysis of K+ channel mutants. J Neurogenet 16(1):45–63

Wang TT, Chen THH, Wang PE, Lai H, Lo MT, Chen PYC, Chiu SYH (2009) A population-based study on the association between type 2 diabetes and periodontal disease in 12,123 middle-aged Taiwanese (KCIS No 21). J Clin Periodontol 36(5):372–379

Wang H, Zhang Q, Chu X, Chen T, Ge J, Yu R (2011) Graphene oxide–peptide conjugate as an intracellular protease sensor for caspase-3 activation imaging in live cells. Angew Chem Int Ed 31(50):7065–7069

Wen Y, Xing F, He S, Song S, Wang L, Long Y, Fan C (2010) A graphene-based fluorescent nanoprobe for silver (I) ions detection by using graphene oxide and a silver-specific oligonucleotide. Chem Commun 46(15):2596–2598

Yan J, Wei T, Shao B, Fan Z, Qian W, Zhang M, Wei F (2010) Preparation of a graphene nanosheet/polyaniline composite with high specific capacitance. Carbon 48(2):487–493

Yang X, Zhang X, Liu Z, Ma Y, Huang Y, Chen Y (2008) High-efficiency loading and controlled release of doxorubicin hydrochloride on graphene oxide. J Phys Chem C 112(45):17554–17558

Yang Y, Liu R, Wu J, Jiang X, Cao P, Hu X, Song Y (2015) Bottom-up fabrication of graphene on silicon/silica substrate via a facile soft-hard template approach. Sci Rep 5(1):13480

Yang T-H, Xirasagar S, Cheng Y-F, Wu C-S, Kao Y-W, Shia B-C, Lin H-C (2020) Malignant otitis externa is associated with diabetes: a population-based case-control study. Ann Otol Rhinol Laryngol 129(6):585–590

Zabihpour T, Shahidi S-A, Karimi-Maleh H, Ghorbani-HasanSaraei A (2020) Voltammetric food analytical sensor for determining vanillin based on amplified NiFe2O4 nanoparticle/ionic liquid sensor. J Food Measure Charact 14(2):1039–1045

Zhang J, Li S, Tang B, Wang Z, Ji G, Huang W, Wang J (2017) High photocatalytic performance of two types of graphene modified TiO 2 composite photocatalysts. Nanoscale Res Lett 12:1–5

Zorov DB, Juhaszova M, Sollott SJ (2014) Mitochondrial reactive oxygen species (ROS) and ROS-induced ROS release. Physiol Rev 94(3):909–950